

# Structural Damage Detection of Truss Bridge under Environmental Variability

Ling Yu<sup>1,2,3,\*</sup> and Junhua Zhu<sup>1,2,4</sup>

<sup>1</sup> MOE Key Lab of Disaster Forecast and Control in Engineering, Jinan University, Guangzhou 510632, China

<sup>2</sup> Science and Technology on Reliability Physics and Application Technology of Electronic Component Laboratory, Guangzhou 510610, China

<sup>3</sup> Department of Mechanics and Civil Engineering, Jinan University, Guangzhou 510632, China

<sup>4</sup> China Electronic Product Reliability and Environmental Testing Research Institute, Guangzhou 510610, China

Received: 5 Dec. 2013, Revised: 6 Apr. 2014, Accepted: 8 Apr. 2014

Published online: 1 Feb. 2015

---

**Abstract:** Focused on the effects of environmental and operational variability on the structures, a novel procedure for structural linear and nonlinear damage detection is proposed based on the time series analysis and the higher statistical moments. The higher statistical moments of residual error of AR model, such as skewness and kurtosis, are then defined as the new damage-sensitive features to be a complimentary. Six integrated damage-sensitive features are further defined for vibration-based damage detection in terms of arithmetic and geometric mean of the residual errors. A series of experiments on a complicated truss bridge combined with a steel bridge plate have been conducted in laboratory. Damage was simulated by loosening the bolts of joints, and environmental variability were introduced by changing the shaker input level. 16 acceleration data of the bridge in each baseline and test state are measured and recorded for the structural damage detection. Based on these time series of acceleration data, the applicability of the proposed procedure is evaluated. Some valued conclusions are made and discussions suggested as well.

**Keywords:** Structural damage detection, time series analysis, fuzzy clustering, statistical moment

---

## 1 Introduction

The vibration-based structural damage detection has received much attention over the past 20 years [1,2]. Most of them can be classified into two groups: model-based and feature based [3]. For the latter, the use of time-domain analysis in constructing time-series signature for direct damage diagnosis has also attracted attention in recent years [4]. As operation in the time domain does not require domain change, it provides a potentially effective alternative for rapid monitoring applications. For the structural health monitoring (SHM), the ideal approach for features extraction is to choose features that are sensitive to damage, but are not sensitive to operational and environmental variations. However, such an approach is not always possible in real-world structures, and intelligent feature extraction procedures are usually required [5]. Fugate et al. [6] fit an autoregressive (AR) model to the measured acceleration-time-histories from an undamaged structure,

defined the residual errors quantifying the difference between the prediction from the AR model and the actual measured time history at each time interval as the damage-sensitive features, and employed X-bar and S control charts are to monitor the mean and variance of the selected features for structural damage detection. Sohn and Farrar [7] proposed a two-step AR-ARX (auto-regressive and auto-regressive with eXogenous) model to predict the time series and subsequently used the standard deviation (STD) ratio of the residual error to indicate the damage. Lu and Gao [4] developed a novel method to construct a novel auto-regressive time-series signature for the diagnosis of structural damage. The model stems from the linear dynamics and is formulated in the form of the ARX model involving only the (acceleration) response data. The STD of the residual error when the reference model is applied on the measured response of an unknown state is used as a damage feature. All of studies mentioned above are based on linear AR or ARX model and assumed the residual

---

\* Corresponding author e-mail: [lyu1997@163.com](mailto:lyu1997@163.com)

error obeys normal distribution. However, this assumption often increase misdiagnosis rate because the damage information main focused on the tails of distribution where slight deviations from the normal condition can be seen. The states with the nonlinearities show that an assumption of normality is not justified [8]. In this paper, a deck-truss bridge structure is designed and fabricated in laboratory for structural damage detection [9], a vibration-based structural damage detection procedure is proposed based on time series analysis, where two higher statistical moments of the residual error of AR model, skewness and kurtosis are adopted to extract the structural damage, two damage-sensitive features are defined as the Skewness and Kurtosis ratio of structural unknown test state to its reference state. Further, six integrated damage-sensitive features are defined in terms of arithmetic and geometric mean meanings. The illustrated results about the structural damage detection of truss bridge demonstrate the applicability of the procedure proposed in this paper.

## 2 Experimental Procedure

**Truss Bridge Description** A deck-truss bridge structure is designed and fabricated in laboratory as shown in Fig. 1, which consists of a bridge deck and six-bay truss structure. The bridge deck is a uniform Q235 steel plate (3100mm × 450mm × 4.5mm) stiffened with five hollow rectangular ribs (30mm × 15mm × 1.9mm) welded under the plate. It is put on the six laterally horizontal tubes of the truss and connected through U-shaped bolts.



Fig. 1 Deck-truss bridge structure

The six-bay 3D truss structure consists of fifty-four stainless steel tubes ( $\phi 22 \times 1.5mm$  thick) jointed together by twenty-four standard Zinc copper alloy ball nodes. Each tube is fitted with a screwed end connector, which, when tightened into the node, also clamps the tube by means of an internal compression fitting. All the connection bolts are tightened with the same torsional moment to avoid asymmetry or nonlinear effects caused

by man-made assembly errors. The length of all the horizontal and vertical tube members between the centers of two adjacent nodes is exactly 500mm, but the length of all diagonal members is 707mm after assembly. The whole deck-truss structure is simple supported at two ends through two ball nodes at each end.

**Experimental Layout** There are twenty-four ball nodes in the truss bridge, in which sixteen nodes are selected to vertically mount PCB ICP 333B30 single axis accelerometers with sensitivity of 100mV/g as shown in Fig. 2. Here, all the blue unilateral arrows represent mounted accelerometers with their direction. An electro-dynamic shaker is vertically attached at the node T23 using a stringer through a PCB ICP 208C02 force sensor with sensitivity of 50mV/lbs. A dark bidirectional arrow indicates it at node T23 in Fig. 2.

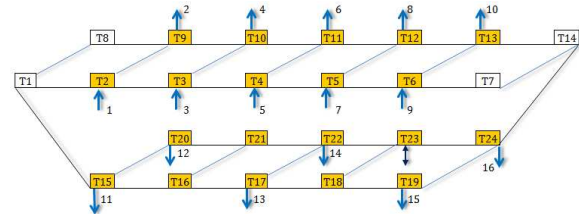


Fig. 2 Layout of 16 accelerometers and one shaker

Table 1 Structural damage scenarios

Bridge state	Description
01H	Baseline (Healthy) state 01
01D	Loosening bolt at the end T2 of T2-T15 tube and then fastening by hand
02D	Completely loosening bolt at the end T2 of T2-T15 tube
03D	Half loosening bolts at two ends of T2-T15 tube
04D	Completely loosening bolts at two ends of T2-T15 tube
05D	Completely loosening bolts at two ends of T2-T15 tube, loosening bolt at the end T21 of T20-T21 tube and then fastening by hand
02H	Healthy state 02, recovered from the damage state 05D

The LMS Vibration Measurement and Modal Analysis system is used to record the acceleration response and excitation force signals with the SCMDAS Mobile Front-End Module SCM05-VB08. The LMS TEST.lab software is used to analyze the sampled data. The data is recorded at a sampling rate of 320Hz. The

**Table 2** Comparison on frequency change ratios under different scenarios

Order	Frequency(Hz)		Frequency Change Ratio(%)				
	01H	01D	02D	03D	04D	05D	02H
1	19.44	-0.376	-2.192	-0.931	-0.931	-0.962	0.010
2	26.01	-0.077	0.031	-0.169	-0.162	-0.138	0.300
3	41.77	-0.730	-2.854	-2.952	-2.775	-2.825	0.429
4	62.26	-0.011	-0.338	-0.450	-0.441	1.649	2.213
5	68.39	-0.181	-0.146	-0.608	-0.554	-0.412	0.465
6	99.84	-0.318	0.128	-0.795	-0.726	-0.775	2.102
7	115.31	-0.014	0.100	-0.004	-0.016	0.251	0.120
8	121.63	-0.129	0.131	-0.278	-0.266	-0.013	0.548
9	134.97	-0.095	0.162	-0.281	-0.265	-0.021	0.705
10	144.19	0.006	-0.029	-0.044	-0.035	-0.078	0.014

excitation band is 0-160Hz. Total sample time period is 99.2s, the length of sample points are 31744.

**Structural Damages** In order to simulate structural damages, five damage scenarios are set up by loosening connection bolts between the node and the tube as shown in Table 1, in which the capital letters H and D represent structural healthy and damage states respectively, cases 01D and 02D are single connection damage, 03D, 04D and 05D are multiple damage with increasing damage extent. It is easy to find that the damage extent is increased with the change in structural states from 01D to 05D. When the excitation level is 1V, the first ten frequencies of the healthy state 01H and the change ratio of frequencies in damage states are listed in Table 2 respectively. It can be seen that most of damages cause the decrease of frequencies but sometimes few increase the frequencies as well when the structure is recovered from the damage state 05D, especial for the fourth and sixth frequencies. This makes the structural damage detection more complicate, it is very difficult to identify the structural damage if only the structural frequencies are only used.

**Table 3** Time series samples in baseline state

Bridge state	Case No	Excitation level (V)	Sample Length	Sample Number
01H	1-5	1	2048	5

**Measured Data** As a baseline state of truss bridge, the measured acceleration responses under the excitation level of 1V are split into 15 samples with a length of 2048 points each. First 5 samples are specified as the reference samples as ones in Table 3, the following 10 samples are specified as the test ones as listed in Table 4. In the same way, 10 acceleration samples with 2048 points each under each of five different excitation levels in various test states are measured and recorded as ones in Table 4. The total sample case number is five for the baseline state in

Table 3, but it is 350 for all the test states as ones in Table 4. It is noted that the first 5 samples in baseline state in Table 3 are different from ones in test state in Table 4 although the case number is the same.

**Environmental Variability** In order to simulate the environmental variability, five excitation levels are set up at each structural state, which are 1V, 3V, 5V, 7V and 9V respectively. Meanwhile, only one measured data at the healthy state 01H is needed to be the reference sample in the mentioned procedure, i.e. any of cases 1-5 in Table 3, all the other data are set to be test sample as listed in Table 4, i.e. case numbers are from 1 to 350 in test states. Here, the first five reference sample data and the test ones are different although both of them are in healthy state 01H.

### 3 Damage Feature Extraction

In this section, damage-sensitive feature extraction procedures are presented based on time-series analysis. Based on linear system theory, AR time series models are used to describe the acceleration time histories and are used in the analysis of stationary time series processes. A stationary process is a stochastic process, one that obeys probabilistic laws, in which the mean, variance and higher order moments are time invariant.

**Measured Data Normalization** In order to eliminate the effects caused by environmental and operational variations from the measured data, the data standardization is necessary as follows

$$\hat{x}_i = \frac{x_i - \bar{x}}{\sigma} \tag{1}$$

$$\bar{x} = \frac{1}{P} \sum_{i=1}^P x_i \tag{2}$$

$$\sigma^2 = \frac{1}{P-1} \sum_{i=1}^P (x_i - \bar{x})^2 \tag{3}$$

**Table 4** Time series samples in test states

Bridge state	Case No	Excitation level (V)
01H	1-10	1
	11-20	3
	21-30	5
	31-40	7
	41-50	9
01D	51-60	1
	61-70	3
	71-80	5
	81-90	7
	91-100	9
02D	101-110	1
	111-120	3
	121-130	5
	131-140	7
	141-150	9
03D	151-160	1
	161-170	3
	171-180	5
	181-190	7
	191-200	9
04D	201-210	1
	211-220	3
	221-230	5
	231-240	7
	241-250	9
05D	251-260	1
	261-270	3
	271-280	5
	281-290	7
	291-300	9
02H	301-310	1
	311-320	3
	321-330	5
	331-340	7
	341-350	9

Notes: Data samples in 02H test states are different from ones in 01H baseline states.

where  $\bar{x}$ ,  $\sigma^2$  and  $\hat{x}_i$  are the mean, variance and standardized version of time series signal  $x_i$ , respectively.

**Traditional Damage-sensitive Feature** AR models attempt to account for the correlations of the current observation in time series with its predecessors. A univariate AR model of order  $p$  at  $j$ -th measured acceleration signal, or AR ( $p$ ), for the time series can be written as

$$A_j(q)x_j(k) = e_j(k) \quad (4)$$

$$A_j(q) = 1 + a_{1j}q^{-1} + a_{2j}q^{-2} + \dots + a_{pj}q^{-p} \quad (5)$$

where  $x_j(k)$  ( $j = 1, 2, \dots, m, k = 1, 2, \dots, n$ ) are the current and previous values of the time series and  $e_j(k)$  is AR model residual error. The AR coefficients  $a_{1j}, a_{2j}, \dots, a_{pj}$  can be evaluated using a variety of methods. Here, the coefficients were calculated using the

Yule-Walker equations [10]. For the structural reference (health) state, the corresponding AR model can be made, the model parameter  $A_j^{ref}(q)$  and residual error  $e_j^{ref}(k)$  can be obtained. Similarly, for any unknown structural test sample  $y_j(k)$ , its residual error is,

$$e_j^{test}(k) = A_j^{ref}(q)y_j(k) \quad (6)$$

If the residual error is assumed as a Gaussian normal distribution with a zero mean, the traditional damage-sensitive feature is defined as the variance ratio of the unknown test state to the reference one as follows [7],

$$Var(e_j) = \frac{\sigma(e_j^{test})}{\sigma(e_j^{ref})} \quad (7)$$

When the test samples come from the structural health state, AR model can effectively predict the sample, therefore the variance of the residual error is close to one of the reference sample, the variance ratio  $Var$  in Eq.(7) is approximately equal to one. When the test samples come from the structural damage state, the residual error will be increased, the variance ratio  $Var$  will be larger than one, therefore, the ratio  $Var$  can be used to determine if the structures are damaged or not.

**Order of AR Model** The order of the AR model is an unknown value. A high-order model may perfectly match the data, but will not generalize to other data sets. On the other hand, a low-order model will not necessarily capture the underlying physical system response. In order to find out the optimum model order, several techniques are used in this study, such as Akaike's information criterion (AIC), partial autocorrelation function (PAF), final prediction error (FPE) etc. Finally, the AIC is selected in this study. The AIC has been used to assess the generalization performance of linear models. In a simple way, this technique returns a value that is the sum of two terms as follows:

$$AIC = -2L_m + 2m \quad (8)$$

Where  $L_m$  is the maximized log-likelihood of the residual error, and  $m$  is the number of adjustable parameters in the model. It assumes a tradeoff between the fit of the model and the model's complexity. The first term is related to how well the model fits the data, i.e., if the model is too simple, the residual errors increase. On the other hand, the second term is a penalty factor related to the complexity of the model, which increases as the number of additional parameters grows [10].

Fig. 3 is the effect of AR order on the AIC of 16 measured accelerations in baseline state. It can be seen that the changes in AIC are very small after AR order is equal to 50, therefore, AR (50) is determined for prediction of the test samples in the following section. Nonlinear damage-sensitive features It should be noted that AR model is a kind of linear model and many classical statistical tests depend on the assumption of



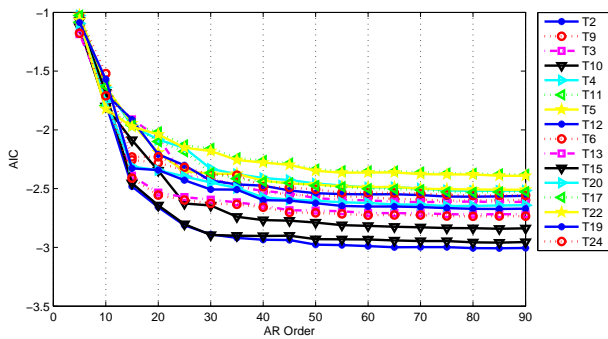


Fig. 3 Determination of AR model order

normality. This approach is based on the assumption that damage will introduce either linear deviation from the baseline condition or nonlinear effects in the signal and, therefore, the linear model developed with the baseline data will no longer accurately predict the response of the damaged system. In order to establish the underlying distribution of the data, some higher statistical moments are used to estimate the probability density function (PDF) of the measured signals without normal distribution. Moreover, it is expected that the damage can introduce significant changes in the acceleration-time-history PDFs and, as a consequence, the third and fourth statistical moments and PDFs are introduced as damage-sensitive features in this study. The third statistical moment is a measure of the asymmetry of the PDF. The normalized third statistical moment is called the skewness and is defined as

$$skewness(e_j) = \frac{E[e_j - m(e_j)]^3}{\sigma^3(e_j)} \tag{9}$$

where a positive skewness means that the right tail is longer and that the area of the distribution is concentrated below the mean. On the other hand, a negative skewness means that the left tail is longer and that the area of the distribution is concentrated above the mean. The skewness of a standard normal distribution is zero. The fourth statistical moment is a measure of the relative amount of data located in the tails of a probability distribution. The kurtosis is the normalized fourth statistical moment and is defined as

$$kurtosis(e_j) = \frac{E[e_j - m(e_j)]^4}{\sigma^4(e_j)} \tag{10}$$

where a kurtosis greater than three indicates a "peaked" distribution that has longer tails than a standard normal distribution. This means that there are more cases far from the mean. Kurtosis less than three indicates a "flat" distribution with shorter tails than a standard normal distribution. This property implies that fewer realizations of the random variable occur in the tails than would be

expected in a normal distribution. The kurtosis of a standard normal distribution is three. Similar to Eq. (7), two damage-sensitive features are defined as the Skewness and Kurtosis ratio of structural unknown test state to its reference state as follows,

$$Skew(e_j) = \left| \frac{skewness(e_j^{est})}{skewness(e_j^{ref})} \right| \tag{11}$$

$$Kur(e_j) = \frac{kurtosis(e_j^{est})}{kurtosis(e_j^{ref})} \tag{12}$$

When the structure is in a health state, the skewness of the AR model residual error is close to zero, its kurtosis approaches to three. But the structure is damaged, the skewness will be positive or negative, the kurtosis will increase. When the test and reference samples come both from same state, the skewness and kurtosis will be identical and equal to one, or else they will be more or less than one, which can be used to detect the damage of structures.

**Integrated Damage-sensitive Features** The damage feature in Eq. (7) is a linear traditional index, Eqs. (11) and (12) are just partial damage-sensitive indexes. In order to integrate their function at the same time, six damage-sensitive features are defined as follows in terms of arithmetic and geometric average meanings,

$$DI_1 = \frac{Var + Skew}{2} \tag{13}$$

$$DI_2 = \frac{Var + Kur}{2} \tag{14}$$

$$DI_3 = \frac{Var + Skew + Kur}{3} \tag{15}$$

$$DI_4 = \sqrt{Var \times Skew} \tag{16}$$

$$DI_5 = \sqrt{Var \times Kur} \tag{17}$$

$$DI_6 = \sqrt[3]{Var \times Skew \times Kur} \tag{18}$$

After the residual error of AR(50) is obtained, all the damage features at each acceleration of 16 channels, i.e. *Var*, *Skew*, *Kur* and six integrated features can be calculated. It can be found from these results that the *Var* features at nodes T9, T2, T20, T15 in the 05D state increase significantly. This is because these nodes are close the damage nodes and the 05D state is the most severe damage state in all damage states, which shows that the *Var* feature can locate the region of damages with some accuracy. In the other states, all the *Var* features do not vary obviously because of the relative small damage in bridge. For the *Skew* and *Kur* features in all test states, both of them vary around the value of one, this is because the residual errors obey the normal distribution and their

nonlinear characteristics are too weak. For the six integrated features, they are affected negatively when the Skew feature is involved, but their whole distribution varies lightly when the *Kur* feature is involved. As a whole, both the features  $DI_2$  and  $DI_5$  are better than the other features. Fig. 4 is the distribution of  $DI_2$  feature. It can be seen that the 05D damage state can be effectively identified.

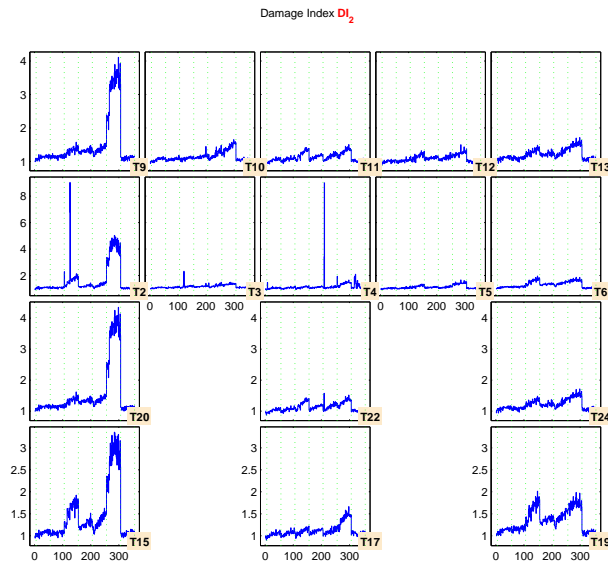


Fig. 4 Distribution of integrated damage feature  $DI_2$

### 4 Structural Damage Detection

In the previous section, damage index has been defined, but it is difficult to choose a threshold values that characterize damage. In order to perform the damage detection, fuzzy c-means clustering (FCM) algorithm, which was first presented by Bezdek [11], and recently applied to SHM problems by da Silva et al. [12], is employed to clarify the features, and supply a fuzzy decision by using the membership of damage index in a cluster. This algorithm is an unsupervised classification algorithm which uses a certain objective function, described in Eq. (19), for iteratively determining the local minima.

$$\min J(C, m) = \sum_{i=1}^C \sum_{j=1}^m u_{ij}^m d_{ij}^2 \tag{19}$$

$$center_i = \frac{\sum_{j=1}^N u_{ij}^m x_j}{\sum_{j=1}^N u_{ij}^m} \tag{20}$$

$$d_{ij}^2 = (x_j - center_i)^T (x_j - center_i) \tag{21}$$

$$u_{ij} = \frac{(d_{ij})^{\frac{-2}{m-1}}}{\sum_{k=1}^C (d_{kj})^{\frac{-2}{m-1}}} \tag{22}$$

where  $C$  is the total number of clusters and  $N$  is the total number of objects in calibration.  $u_{ij}$  is the membership function associated with the  $j$ -th object of the  $i$ -th cluster, which is updated by using Eq. (22) in each iteration step. The exponent  $m$  is a measurement of fuzzy partition.  $center_i$  is the centroid of the  $i$ -th cluster,  $x_j$  is  $j$ -th object of data set to be clustered, which is set to be any of damage-sensitive features here,  $d_{ij}$  denotes the distance between  $j$ -th object and the centroid of the  $i$ -th cluster, here, Euclidean distance is used as Eq. (21) [13].

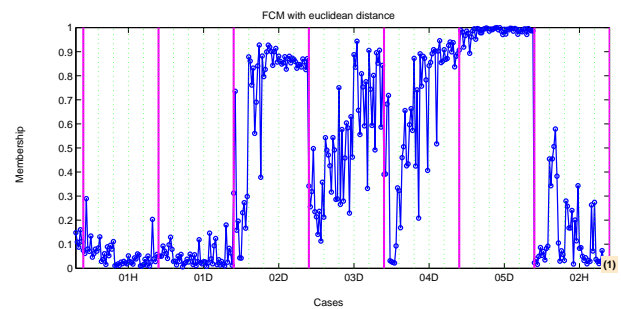


Fig. 5 Damage detection using FCM of integrated damage feature  $DI_2$

Fig. 5 shows the structural damage detection results of total 350 test states based on FCM of integrated damage feature  $DI_2$ . It can be found that most of damage states can be effectively identified except for the weaker 01D damage state. The results under the light excitation level are worse relatively. Although there is weaker nonlinear for all the acceleration responses, considering the skewness feature does not affect the detection results negatively. By contraries, it possibly causes wrong diagnosis if the higher statistical moments are not considered. The illustrated results show that the kurtosis feature is more effective between the skewness and kurtosis features.

### 5 Conclusions

A novel vibration-based structural damage detection procedure is proposed based on time series analysis and higher statistical moments in this paper. A deck-truss bridge structure is designed and fabricated in laboratory for structural damage detection. Some higher statistical moments of the residual error of AR model, such as skewness and kurtosis, are adopted to extract the structural damage features, two damage-sensitive features are defined as the Skewness and Kurtosis ratio of

structural unknown test state to its reference state respectively. Six integrated damage-sensitive features are further defined in terms of arithmetic and geometric mean meanings. The illustrated results on the truss bridge show that most of structural damages can be effectively identified by the vibration-based damage detection procedure proposed here. However, although there is weaker nonlinear for all the acceleration responses of bridge, considering the skewness feature does not affect the detection results negatively. By contraries, it possibly causes misdiagnosis if the higher statistical moments are not taken into account.

## Acknowledgements

This research work is jointly supported by the National Natural Science Foundation of China (50978123, 51278226 and 11032005), Guangdong Natural Science Foundation (10151063201000022), the Fundamental Research Funds for the Central Universities (21611512) and the Opening Project of Science and Technology on Reliability Physics and Application Technology of Electronic Component Laboratory (No. ZHD201207).

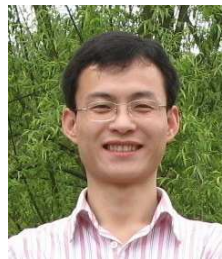
## References

- [1] Y. J. Yan, L. Cheng, Z. Y. Wu and L. H. Yam, Development in vibration-based structural damage detection technique, *Mechanical System and Signal Processing*, **21**, 2198-2211, (2007).
- [2] E. P. Carden and F. Fanning, Vibration based condition monitoring: a review, *Structural Health Monitoring*, **3**, 355-377, (2004).
- [3] Q. W. Zhang, Statistical damage identification for bridges using ambient vibration data, *Computers and Structures*, **85**, 476-485, (2007).
- [4] Y. Lu and F. Gao, A novel time-domain auto-regressive model for structural damage diagnosis, *Journal of Sound and Vibration*, **283**, 1031-1049, (2005).
- [5] K. Worden, C. R. Farrar, G. Manson and G. Park, The Fundamental Axioms of Structural Health Monitoring, *Proceedings of the Royal Society*, **463**, 1639-1664, (2007).
- [6] M. L. Fugate, H. Sohn and C. R. Farrar, Vibration-based damage detection using statistical process control, *Mechanical Systems and Signal Processing*, **15**, 707-721, (2001).
- [7] H. Sohn, C. R. Farrar, Damage diagnosis using time series analysis of vibration signals, *Smart Materials and Structures*, **10**, 1-6, (2001).
- [8] E. Figueiredo, G. Park, J. Figueiras, C. R. Farrar and K. Worden, Structural Health Monitoring Algorithm Comparisons Using Standard Data Sets, Los Alamos National Laboratory Report, LA-14393, (2009).
- [9] L. Yu, J. H. Zhu and L. L. Yu. Structural damage detection in a truss bridge model using fuzzy clustering and measured FRF data reduced by principal component projection, *Advances in Structural Engineering*, **16**, 207-217, (2013).
- [10] G. Box and G. Jenkins, *Time Series Analysis: Forecasting and Control*, Prentice Hall, Englewood Cliffs, New Jersey, (1976).
- [11] J. C. Bezdek, *Pattern recognition with fuzzy objective function algorithm*, Plenum Press, NY, (1981).
- [12] S. da Silva, M. Dias Jnior, V. Lopes Junior and M. J. Brennan, Structural damage detection by fuzzy clustering, *Mechanical System and Signal Processing*, **22**, 1636-1649, (2008).
- [13] MATLAB: Toolbox user's guide. <http://www.mathworks.com/products/>, The MathWorks, Inc. (2000).



**Ling Yu** received B.S. degree in Helicopter Engineering and M.S. in Solid Mechanics both from the Nanjing University of Aeronautics and Astronautics and Ph.D. degree in Structural Engineering from the Hong Kong Polytechnic University.

He is a full professor at Jinan University. His research interests focus on structural dynamics and vibration, moving loads problems, system identification and applications to SHM, etc..



**Junhua Zhu** received B.S. degree in Prospecting Engineering from Jilin University, M.S. degree in Geotechnical Engineering from Changjiang River Scientific Research Institute, and Ph.D. degree in Engineering Mechanics from Jinan University. He is

currently an engineer at China Electronic Product Reliability and Environmental Testing Research Institute. His research interests focus on the reliability assessment of mechanical and electronic products.